RESEARCH ARTICLE | AUGUST 30 2022

# Ultrafast modulation of a THz metamaterial/graphene array integrated device

Abdullah M. Zaman ; Yuichi Saito ; Yuezhen Lu ; Farhan Nur Kholid ; Nikita W. Almond;
Oliver J. Burton; Jack Alexander-Webber ; Stephan Hofmann ; Thomas Mitchell; Jonathan D. P. Griffiths;
Harvey E. Beere; David A. Ritchie ; Rostislav V. Mikhaylovskiy ; Riccardo Degl'Innocenti

Check for updates

View Online    Export Citation

# Ultrafast modulation of a THz metamaterial/graphene array integrated device

Abdullah M. Zaman,[1,2] [iD] Yuichi Saito,[3] [iD] Yuezhen Lu,[1] [iD] Farhan Nur Kholid,[3] [iD] Nikita W. Almond,[4]
Oliver J. Burton,[5] Jack Alexander-Webber,[5] [iD] Stephan Hofmann,[5] [iD] Thomas Mitchell,[4] Jonathan D. P. Griffiths,[4]
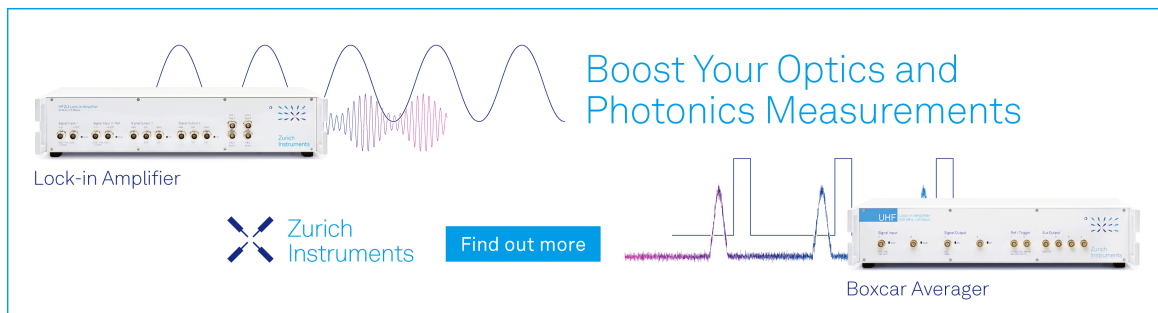Harvey E. Beere,[4] David A. Ritchie,[4] [iD] Rostislav V. Mikhaylovskiy,[3] [iD] and Riccardo Degl'Innocenti[1,a] [iD]

## AFFILIATIONS

[1]Department of Engineering, University of Lancaster, Bailrigg, Lancaster LA1 4YW, United Kingdom
[2]College of Engineering, Taibah University, Madina 42353, Saudi Arabia
[3]Department of Physics, University of Lancaster, Bailrigg, Lancaster LA1 4YW, United Kingdom
[4]Cavendish Laboratory, University of Cambridge, J. J. Thomson Avenue, Cambridge CB3 0HE, United Kingdom
[5]Department of Engineering, University of Cambridge, 9 J. J. Thomson Avenue, Cambridge CB3 0FA, United Kingdom

[a]Author to whom correspondence should be addressed: r.deglinnocenti@lancaster.ac.uk

## ABSTRACT

We report on the ultrafast modulation of a graphene loaded artificial metasurface realized on a $SiO_2/Si$ substrate by near-IR laser pump, detected via terahertz probe at the resonant frequency of $\sim$0.8 THz. The results have been acquired by setting the Fermi energy of graphene at the Dirac point via electrostatic gating and illuminating the sample with 40 fs pump pulses at different fluences, ranging from 0.9 to 0.018 mJ/cm$^2$. The sub-ps conductivity rising time was attributed to the combined effect of the ultrafast generation of hot carriers in graphene and electron–hole generation in silicon. In correspondence of the resonance, it was possible to clearly distinguish a partial recovery time of $\sim$2 ps mainly due to carrier-phonon relaxation in graphene, superimposed to the > 1 ns recovery time of silicon. The resonant meta-surface yielded $\sim$6 dB modulation depth in E-field amplitude at 0.8 THz for the range of fluences considered. These measurements set an upper limit for the reconfiguration speed achievable by graphene-based terahertz devices. At the same time, this work represents a great progress toward the realization of an ultrafast THz optoelectronic platform for a plethora of applications, ranging from the investigation of the ultrastrong light-matter regime to the next generation wireless communications.

Research in metamaterial integrated devices operating in the terahertz (THz) range, broadly defined between 0.1 and 10 THz, has reported an exceptionally fast growth in recent years, driven by the unique and strategical applications at these frequencies, such as spectroscopy, imaging, and communications.[1–3] In particular, for the next generation wireless communications (6G), the constant need for an unallocated frequency range inevitably pushes research toward the THz regime. 6G technology includes augmented reality, medical imaging, rack-to-rack communications in supercomputers, satellite communications, kiosk downloading, and indoor links. These are all hungry data-rate applications.[4–7] Metamaterials[8,9] are subwavelength artificial atoms capable to yield an artificial electromagnetic resonant response in the permittivity and/or permeability. These resonances depend on the metamaterial shape and size rather than the materials of choice, thus allowing for a large variety of designs and high efficiency over the whole spectral range. Among the plethora of approaches developed in the latest years for the modulation of THz radiation in this traditionally difficult frequency range to work in, only a limited few have the potential to achieve a benchmark of 100 Gbps–1 Tbps, as dictated by next generation wireless communication.[1] The CMOS technology is the most mature technology reporting high modulation depths and a few GHz speed[10] in the subterahertz frequency range, and it is not foreseeable a further expansion toward higher frequencies, due to the well-known reduced efficiency of electronics approaches. Phase change materials[11] or microelectromechanical systems (MEMS)[12] are known to report high modulation depths but have intrinsically low reconfiguration speeds. Bidimensional electron gases (2DEG) and semiconductor approaches in general reported all electronically high modulation speed in waveguide[13] as well as in compact array devices.[14,15] Finally, 2D materials such as graphene

reported lately[16] similar figures of merit. The integration of graphene, as active material, with metamaterial resonators has proved to be successful in the realization of amplitude,[17,18] frequency,[19,20] and polarization modulators.[21–23] Recently, we reported on the all-electronic modulation of the metamaterial/graphene arrays with >3GHz reconfiguration speed, only limited by the available instrumentation with >7dB amplitude modulation depth around 800 GHz.[16] Optical pump THz probe (OPTP) has been widely used to investigate the excitation and relaxation processes of semiconductors, e.g., silicon,[24–27] as well as of graphene.[28–31] At the same time, all-optical approaches aiming to the realization of THz modulation with metamaterials have been reported in a plethora of configurations, including germanium,[32,33] silicon,[34,35] LT-GaAs,[36] and other active materials such as perovskites.[37] The recorded full duty cycle modulation times vary from the 2–3 ps reported in Refs. 32 and 36 to ∼20 ps for perovskites[37] to hundreds of ps for sub-micrometer silicon patches shunting metallic rings.[34] The picture of carrier dynamics in silicon is well-acquainted, while graphene excitation and relaxation processes are more complex and critically depend on the Fermi energy position. Despite the intrinsic difficulties connected with performing OPTP onto a strongly absorbing substrate (silicon's bandgap is ∼1.12 eV, while the typical femtosecond laser pump wavelength is centered around 780 nm), the graphene excitation and relaxation dynamics could be resolved, yielding a ∼2 ps timescale, depending on the impinging fluence in correspondence of the device's resonance, which is in excellent agreement with the reported literature. This work reinforces the use of graphene as an active medium for achieving ultrafast all-optical THz modulation reporting a total reconfiguration time among the fastest recorded. These measurements reveal an intrinsic physical limitation to the modulation speed achievable by graphene/metamaterial integrated devices.

The optical pump THz probe (OPTP) arrangement and device's architecture are schematically shown in Fig. 1. The metamaterial/graphene array device, as reported in Ref. 16, was fabricated on top of a commercially available $SiO_2$/Si (300 nm/500 $\mu$m) substrate. The Si substrate is a slightly p-doped wafer, to allow back gating. Details on the modulator's structure are illustrated in Fig. 1(a). Source, drain, and top gate connections are also reported in Figs. 1(a) and 1(b), as the device can be used as an ultrafast graphene detector as well. The device can be operated with either top-gate or back-gate. Back-gating is less susceptible to leakage currents, while the top-gate configuration requires lower voltage, and it is necessary for ultrafast all-electronical operation of the device. The total size of the array is $1.3 \times 1.2$ mm$^2$, and it comprises 440 identical interdigitated split-ring (SR) units electrically connected in a nested arrangement, as shown in Figs. 1(b) and 1(c). This architecture follows the design proposed in Refs. 14 and 15, for 2DEG, and yields an increased modulation depth, thanks to the dynamic shift between collective to single unit optical response. The fabrication process begins with a graphene monolayer grown via chemical vapor deposition (CVD) and transferred on top of $SiO_2$/Si samples.[38] Graphene is then patterned into an array of rectangular features ($13 \times 16$ $\mu$m$^2$ size) by using optical lithography followed by $O_2$ RF plasma etching. The SRs shunting the graphene areas are patterned using a photolithography step followed by Ti/Au thermal evaporating (10 nm/150 nm) and liftoff. The SRs along with the graphene patches are encapsulated by a 150 nm thick $Al_2O_3$ layer deposited via atomic layer deposition (ALD). The encapsulation of graphene via ALD serves
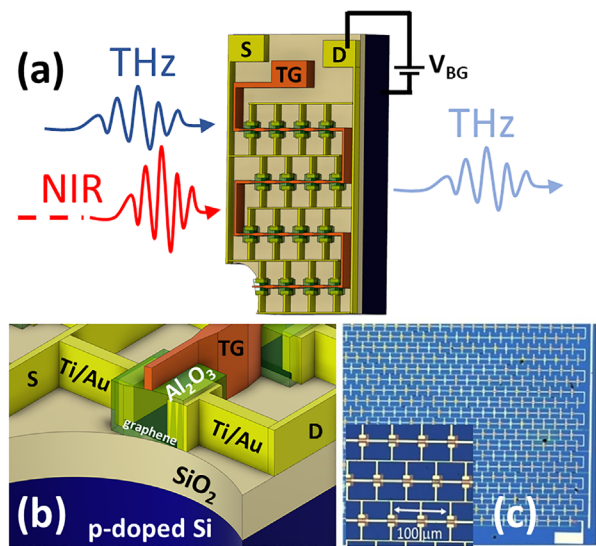


**FIG. 1.** (a) Schematic of the OPTP experimental arrangement where the MM/graphene sample was kept at the Dirac point by acting on the back-gate voltage ($V_{BG}$). S, D, and TG represent the source, drain, and top gate of the device, respectively. (b) Cross section of the device and (c) optical picture of the top surface.

many purposes. In the first place, it allows to design a top gate centered in the SRs' capacitance gaps required in order to achieve a fast, all-electronic modulation.[16] This gate was realized via electron beam lithography followed by Ti/Au thermal evaporation (10/120 nm) and liftoff. The gaps' distance was nominally 7.5 $\mu$m, and the top gate width reduced to 1.5 $\mu$m in correspondence of the resonant elements. At the same time, ALD encapsulation protects graphene and helps bringing the Dirac point at lower voltages and reducing hysteresis.[39,40] The OPTP setup used a Solstice femtosecond laser from Spectra Physics with 40 fs pulse duration and 1 kHz repetition rate at 800 nm central wavelength. The THz pulses were generated by using 1 mm-thick ⟨110⟩ ZnTe, and a similar ZnTe crystal was used in the electro-optic sampling for time-resolved detection. A mechanical stage was allowed to introduce a delay of >1 ns between the collinear pump and probe pulses, with a ∼40 fs pulse resolution. The sample was placed in the focal point of an optical system based on 90° gold coated parabolic mirrors with ∼5 cm focal length. The pump spot size illuminating the sample was set to 2.1 mm diameter by using suitable irises, while the THz spot was measured to be approximately 1 mm. This laser system was used to investigate two different areas on the same sample. The first one is the MM/graphene array presented in Fig. 1. The second one is an area with similar size but with continuous graphene monolayer, without any metallic structure or dielectric layer, which was used for normalization and control. The THz transmitted pulses were recorded at different relative delays with respect to the pump pulses, and the pump fluences were varied by using a set of neutral density filters. The polarization of the THz pulse was always kept linear and perpendicular to the SRs' gaps, in order to excite the MM response at 0.8 THz. Finally, the MM/graphene array was always kept at +30 V, corresponding to the Dirac point and to the maximum of the resonance. This is fundamental in order to ensure that the main effect of the pump induced change is a

positive increase in the graphene's carrier density, and hence conductivity, rather than an increase in the scattering time, which would conversely have a negative correlation with the fluence and was observed for highly doped samples.[28,29]

The intrinsic difficulty in this work consisted in retrieving the graphene pump induced changes on top of the larger effect of the doped silicon substrate. In particular, in the MM array, graphene areas are greatly reduced compared to the illuminated spot size. After having carefully positioned the sample in the focus of the optical system, preliminary measurements were performed on the uniform graphene area, as shown in Fig. 2. Figure 2(a) reports the maximum of the E-field temporal pulse at different delays for a near infrared fluence of 0.18 mJ/cm$^2$ compared to other substrates without graphene, e.g., SiO$_2$/Si (doped), SiO$_2$/Si (undoped), and Si (doped). The different curves have been opportunely shifted in time and normalized to ease the comparison. The steep, sub-ps decrease in the E-field intensity is appreciated in all the curves, opportunely scaled to ease comparison, but only the black trace showed a more complex feature, a reproducible <2 ps dip on top of the predominant absorption in silicon. This was attributed to the presence of graphene. The transmission curves acquired at different delays for a fluence $\Phi = 0.18$ mJ/cm$^2$ for the uniform graphene samples are presented in Fig. 2(b) and are predominantly attributed to the carriers' generation and recombination in silicon. The sub-picosecond fast decrease in transmission and the lack of a full recovery after > 300 ps (not observed even after 1 ns at the maximum delay allowed by the delay stage in other measurements, not presented here) are consistent with literature.[24–27] The MM/graphene array was then positioned in the focus of the THz beam and its transmission recorded for various pump fluences, ranging from $\Phi$ = 0.9 to $\Phi = 0.018$ mJ/cm$^2$ by acting on a set of neutral filters, always keeping the device at Dirac point by providing a constant voltage of +30 V through a Keithley (model 2450) source-meter. The results recorded after a relative pump/probe delay of 200 fs are reported in Fig. 3(a) for different fluences. The 200 fs delay was chosen as it

includes the contributions to conductivity arising from both silicon and graphene. There is a clear resonance observed at around 0.75 THz, which is completely smeared out at higher fluences. This is expected as the pump induced conductivity change strongly dampens the resonant mode, by increasing the carriers in the graphene area shunting the gaps of the SR array, and by acting on the Si conductivity and absorption. The SR subwavelength mode is significantly overlapping with the substrate; therefore, the two effects are present at the same time, even though on a different timescale. Figure 3(b) shows the evolution of the THz transmitted signal for $\Phi = 0.18$ mJ/cm$^2$. The delay timescale is limited to 30 ps as further delays do not add significant information to the picture. The resonance is fully damped after a few ps. At the same time, the whole THz transmitted spectrum out of the resonance is following a similar but not identical trend. Similar transmission sets were acquired for different fluences and are reported in Fig. S1 in the supplementary material. The modulation depth defined as the difference between the THz amplitudes at resonance and at 1.2 THz [as shown by the red dotted arrows in Fig. 3(a)] reports approximately 6 dB dynamic range when comparing the curve acquired before the pump with the ones acquired after a few ps in Fig. S1(a). These results are in very good agreement with the all-electronic measurements acquired with a different THz-TDS setup and reported in the supplementary material in Fig. S2. In order to investigate the effect of graphene induced conductivity from the overall induced absorption in silicon, the modulation depth was extracted from the OPTP datasets previously acquired. The results are shown in Fig. 4. Differently from the results obtained for the graphene continuous area (black trace), where the predominant effect from the silicon hinders the observation of carrier dynamics in graphene, the strong SR array resonance and its extreme sensitivity to changes in the graphene conductivity allow to observe a reproducible trend. The curves have been scaled to ease reading. The graphene conductivity increases under the effect of optical pumping, as expected,[28] since the sample was kept with the Fermi energy fixed at the Dirac point. The retrieval
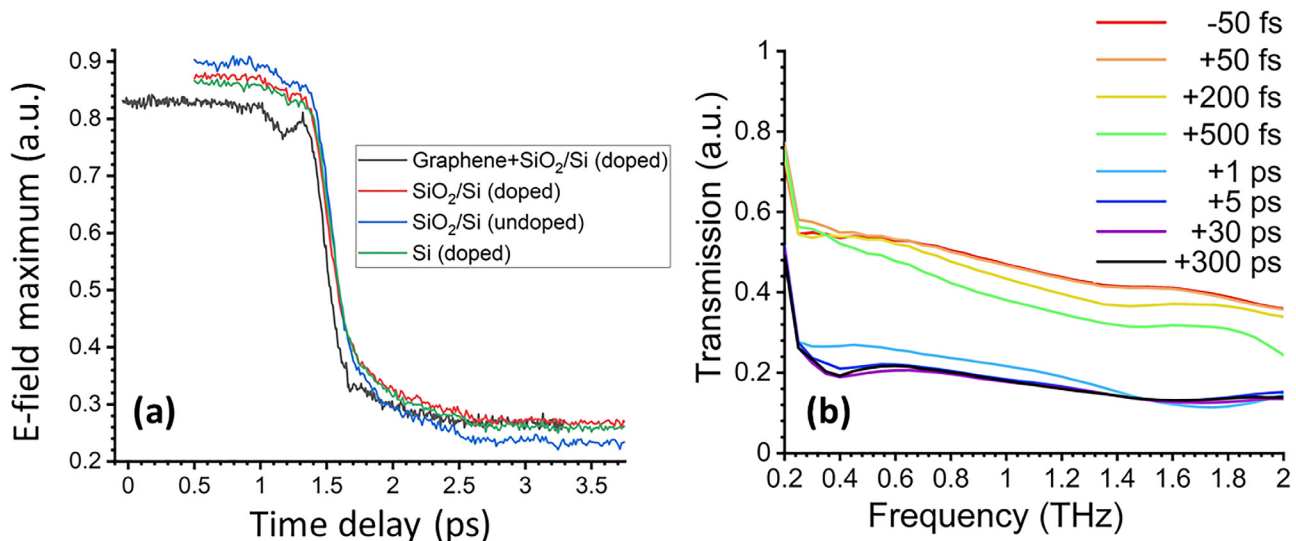


**FIG. 2.** (a) Maximum THz E-field transmitted as a function of the time delay with respect to the pump pulse with fluence $\Phi = 0.18$ mJ/cm$^2$ for different materials. (b) THz transmission for the same pump fluence at different delays through the graphene uniform area on top the SiO$_2$/Si substrate.
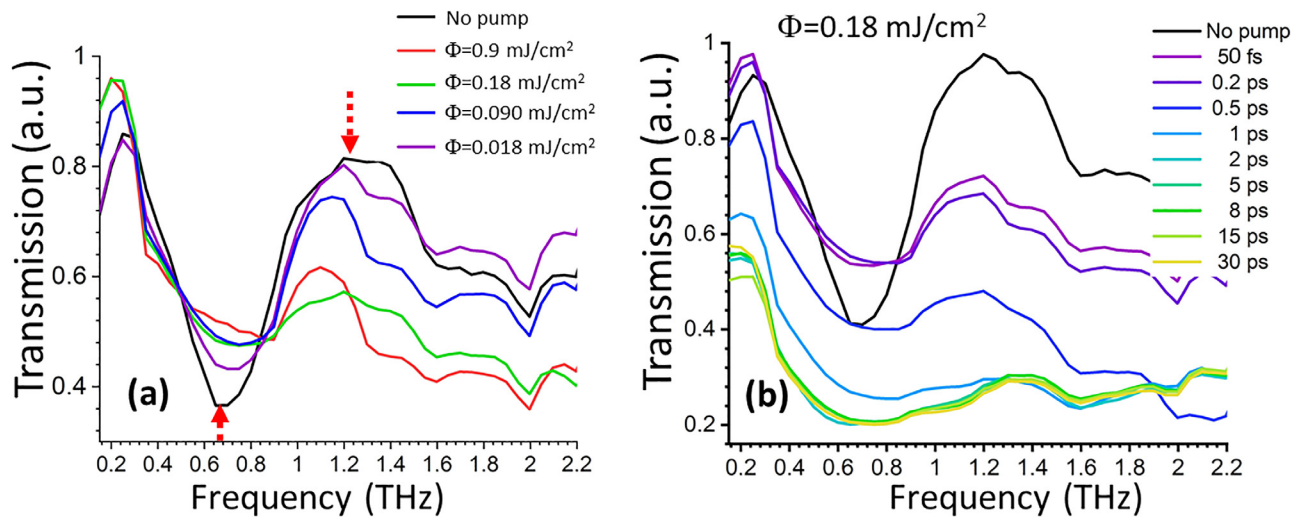
**FIG. 3.** (a) MM/graphene THz transmission for different pump fluences, recorded at 200 fs time delay. (b) THz transmission curves acquired at different time delays with a pump fluence of 0.18 mJ/cm$^2$.

of the precise time evolution due to the graphene effect requires a precise modeling of the fluence dependent silicon carriers' dynamics, graphene excitation, and recombination times, convoluted with the laser pulse width. This investigation, though feasible, necessitates of significant larger datasets. Further to this, the task is beyond the purpose of this manuscript, which is not centered on the retrieval of graphene time-resolved conductivity changes, rather focused on the investigation of the ultimate time limit of a graphene-based MM device for THz ultrafast modulation. It was preferred to provide an upper limit in the time dynamics attributed to graphene, by assuming a laser pulse limited width in the ultrafast excitation of the carriers as
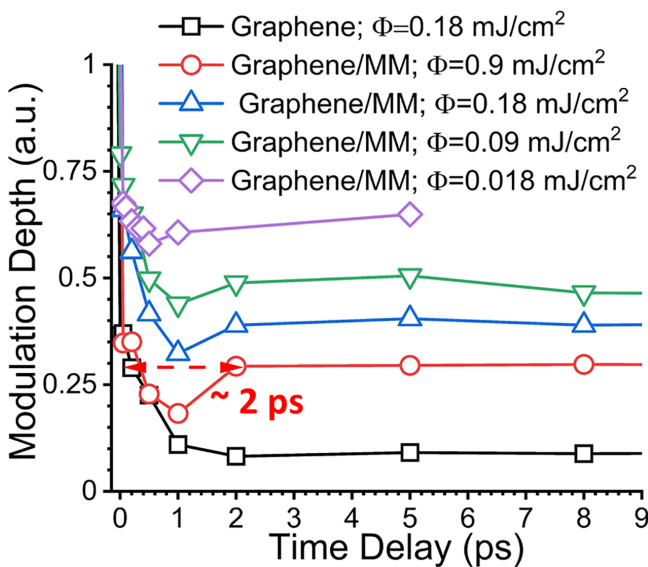
shown in Fig. 4, where the total time cycle is reported for the highest fluence $\Phi = 0.9$ mJ/cm$^2$. A recovery, hence a decrease in conductivity transducing into an increase in the modulation depth, is observed in about ~2 ps, in very good agreement with the reported literature value of ~1.9 ps.[28] Lower fluences tend to have shorter cycles, with the lowest one, 0.018 mJ/cm$^2$, yielding almost sub-picosecond recovery time, as already observed in Refs. 29, 30. The ultrafast decrease in the modulation depth in graphene is attributed to ultrafast generation of hot carrier distribution, which mainly relaxes on timescale of hundreds of fs by carrier–carrier scattering, followed by carrier–phonon scattering and electron–hole recombination, which are the main processes for times >1 ps.[41] Graphene excitation and relaxation dynamics are observed on top of a large background arising from the photogenerated carriers in silicon, thanks for the strong light concentration provided by the resonant mode. It is worth highlighting that these measurements were performed on a complex device, where graphene areas are encapsulated in dielectric and implemented in a double electrical gate metamaterial array. Yet, graphene dynamics are ultimately determining the optoelectronic response of the devices, and they could be retrieved despite using optical pumping above the silicon gap. The complex fabrication did not seem to have affected the graphene properties, which are consistent with the OPTP measurements previously reported.[28–30] This work reinforces the suitability of OPTP for THz optoelectronic device investigation beyond the bare material study and provides an upper intrinsic limit of the maximum reconfiguration speed of these devices. Finally, these results show the suitability of graphene for ultrafast THz photonic applications, such as the realization of the deep, strong light-matter regime for the investigation of exotic quantum phenomena.[42] In order to fully appreciate and model the device dynamics, it is envisaged that the contribution on silicon to the total induce conductivity should be drastically reduced. The first route consists in optical pumping below the Si gap, which would allow us to further increase the analysis on graphene optical pumping as well. Alternative solution consists in using a different substrate but would



**FIG. 4.** Modulation depths vs time delays calculated for different pump fluences.

require changing the device architecture, novel device fabrication, and using a platform other than silicon.

In conclusion, this work reported the ultrafast modulation of an MM array loaded with graphene at the resonance frequency of ∼0.8 THz by using the OPTP laser system and controlling electronically at the same time the graphene's Fermi level at the Dirac point. The modulation depth reported, ∼6 dB in power, is in very good agreement with the >7 dB reported all-electronically. By suitably calibrating the impinging fluence of the optical pump, it was possible to discern the induced conductivity dynamics in the silicon substrate from the graphene ones, which were recorded to be ∼2 ps in very good agreement with previous literature reported on graphene. These results reinforce the use of metamaterial/graphene optoelectronic devices for the ultrafast modulation of terahertz waves.

See the supplementary material for further OPTP transmission curves acquired for different pump fluences; all-electronic modulation of the metamaterial/graphene transmission acquired with a commercial fiber-coupled THz time domain spectrometer; and finite element method simulations of the device transmission calculated for different graphene conductivity.

## AUTHOR DECLARATIONS
### Conflict of Interest

The authors have no conflicts to disclose.

### Author Contributions

**Abdullah M. Zaman:** Conceptualization (equal); Data curation (equal); Formal analysis (equal); Investigation (equal); Methodology (equal); Software (equal); Writing – original draft (equal); Writing – review and editing (equal). **J. P. Griffiths:** Resources (supporting); Writing – review and editing (supporting). **Harvey E. Beere:** Conceptualization (supporting); Funding acquisition (supporting); Investigation (supporting); Methodology (supporting); Resources (supporting); Supervision (supporting); Writing – review and editing (supporting). **David A. Ritchie:** Conceptualization (supporting); Funding acquisition (supporting); Investigation (supporting); Methodology (supporting); Resources (supporting); Supervision (supporting); Writing – review and editing (supporting). **Rostislav V. Mikhaylovskiy:** Conceptualization (equal); Formal analysis (supporting); Funding acquisition (equal); Investigation (equal); Methodology (equal); Resources (equal); Supervision (equal); Validation (supporting); Writing – original draft (supporting); Writing – review and editing (equal). **Riccardo Degl'Innocenti:** Conceptualization (lead); Data curation (equal); Formal analysis (lead); Funding acquisition (equal); Investigation (equal); Methodology (equal); Resources (equal); Software (supporting); Supervision (equal); Writing – original draft (equal); Writing – review and editing (lead). **Yuichi Saito:** Conceptualization (equal); Data curation (equal); Formal analysis (equal); Investigation (equal); Methodology (equal); Software (lead); Validation (supporting); Writing – original draft (equal); Writing – review and editing (equal). **Yuezhen Lu:** Data curation (supporting); Formal analysis (supporting); Investigation (equal); Methodology (supporting); Software (supporting); Validation (equal); Visualization (equal); Writing – original draft (supporting); Writing – review and editing (supporting). **Farhan Nur Kholid:** Conceptualization (supporting); Data curation (supporting); Formal analysis (supporting); Investigation (supporting); Methodology (supporting); Resources (supporting); Supervision (supporting); Validation (supporting); Writing – original draft (supporting); Writing – review and editing (supporting). **Nikita Almond:** Data curation (supporting); Investigation (supporting); Methodology (supporting); Resources (equal); Writing – original draft (supporting); Writing – review and editing (supporting). **Oliver Burton:** Investigation (supporting); Methodology (supporting); Resources (equal); Writing – review and editing (supporting). **Jack Alexander-Webber:** Conceptualization (supporting); Funding acquisition (supporting); Investigation (supporting); Methodology (supporting); Resources (equal); Writing – review and editing (supporting). **Stephan Hofmann:** Conceptualization (equal); Data curation (equal); Funding acquisition (equal); Investigation (equal); Methodology (equal); Resources (equal); Supervision (supporting); Writing – original draft (supporting); Writing – review and editing (supporting). **Thomas A. Mitchell:** Resources (supporting); Writing – review and editing (supporting).

## DATA AVAILABILITY

The data that support the findings of this study are openly available in Lancaster University's PURE at https://doi.org/10.17635/lancaster/researchdata/544, Ref. 43.

## REFERENCES

[1] R. Degl'Innocenti, H. Lin, and M. Navarro-Cía, "Recent progress in terahertz metamaterial modulators," Nanophotonics **11**, 1485–1514 (2022).

[2] Z. Yaxin, Z. Hongxin, K. Wei, W. Lan, D. M. Mittleman, and Y. Ziqiang, "Terahertz smart dynamic and active functional electromagnetic metasurfaces and their applications," Philos. Trans. R. Soc., A **378**, 20190609 (2020).

[3] S. Shen, X. Liu, Y. Shen, J. Qu, E. Pickwell-MacPherson, X. Wei, and Y. Sun, "Recent advances in the development of materials for terahertz metamaterial sensing," Adv. Opt. Mater **10**, 2101008 (2022).

[4] Z. T. Ma, Z. X. Geng, Z. Y. Fan, J. Liu, and H. D. Chen, "Modulators for terahertz communication: The current state of the art," Research **2019**, 6482975.

[5] T. Nagatsuma, G. Ducournau, and C. Renaud, "Advances in terahertz communications accelerated by photonics," Nat. Photonics **10**, 371–379 (2016).

[6] H. Elayan, O. Amin, B. Shihada, R. M. Shubair, and M. S. Alouini, "Terahertz band: the last piece of RF spectrum puzzle for communication systems," IEEE Open. J. Commun. Soc. **1**, 1–32 (2020).

[7] F. Yang, P. Pitchappa, and N. Wang, "Terahertz Reconfigurable Intelligent Surfaces (RISs) for 6G communication links," Micromachines **13**, 285 (2022).

[8] S. Lee, S. Baek, T. T. Kim, H. Cho, S. Lee, J. H. Kang, and B. Min, "Metamaterials for enhanced optical responses, and their application to active control of terahertz waves," Adv. Mater. **32**, 2000250 (2020).

[9] H. T. Chen, A. J. Taylor, and N. Yu, "A review of metasurfaces; physics and applications," Rep. Prog. Phys. **79**, 076401 (2016).

[10] S. Venkatesh, X. Lu, H. Saeidi, and K. Sengupta, "A high-speed programmable and scalable terahertz holographic metasurface based on tiled CMOS chips," Nat. Electron. **3**, 785–793 (2020).

[11] P. Pitchappa, A. Kumar, S. Prakash, H. Jani, T. Venkatesan, and R. Singh, "Chalcogenide phase change material for active terahertz photonics," Adv. Mater. **31**, 1808157 (2019).

21 May 2024 05:37:14

[12]P. Pitchappa, A. Kumar, H. Liang, S. Prakash, N. Wang, A. A. Bettiol, T. Venkatesan, C. Lee, and R. Singh, "Frequency-agile temporal terahertz metamaterials," Adv. Opt. Mater. **8**, 2000101 (2020).

[13]D. Shrekenhamer, S. Rout, A. C. Strikwerda, C. Bingham, R. D. Averitt, S. Sonkusale, and W. J. Padilla, "High speed terahertz modulation from metamaterials with embedded high electron mobility transistors," Opt. Express **19**, 9968–9975 (2011).

[14]Y. Zhang, S. Qiao, S. Liang, Z. Wu, Z. Yang, Z. Feng, H. Sun, Y. Zhou, L. Sun, Z. Chen, X. Zou, B. Zhang, J. Hu, S. Li, Q. Chen, L. Li, G. Xu, Y. Zhao, and S. Liu, "Gbps terahertz external modulator based on a composite metamaterial with a double-channel heterostructure," Nano Lett. **15**, 3501–3506 (2015).

[15]Y. Zhao, L. Wang, Y. Zhang, S. Qiao, S. Liang, T. Zhou, X. Zhang, X. Guo, Z. Feng, F. Lan, Z. Chen, X. Yang, and Z. Yang, "High-speed efficient terahertz modulation based on tunable collective-individual state conversion within an active 3 nm two-dimensional electron gas metasurface," Nano Lett. **19**, 7588–7597 (2019).

[16]A. M. Zaman, Y. Lu, X. Romain, N. W. Almond, O. J. Burton, J. Alexander-Webber, S. Hofmann, T. Mitchell, J. D. P. Griffiths, H. E. Beere, D. A. Ritchie, and R. Degl'Innocenti, "Terahertz metamaterial optoelectronic modulators with GHz reconfiguration speed," IEEE Trans. Terahertz Sci. Technol. (published online, 2022).

[17]D. S. Jessop, S. J. Kindness, L. Xiao, P. Braeuninger-Weimer, H. Lin, Y. Ren, C. X. Ren, S. Hofmann, J. A. Zeitler, H. E. Beere, D. A. Ritchie, and R. Degl'Innocenti, "Graphene based plasmonic terahertz amplitude modulator operating above 100 MHz," Appl. Phys. Lett. **108**, 171101 (2016).

[18]S. J. Kindness, D. S. Jessop, B. Wei, R. Wallis, V. S. Kamboj, L. Xiao, Y. Ren, P. Braeuninger-Weimer, A. I. Aria, S. Hofmann, H. E. Beere, D. A. Ritchie, and R. Degl'Innocenti, "External amplitude and frequency modulation of a terahertz quantum cascade laser using metamaterial/graphene devices," Sci. Rep. **7**, 7657 (2017).

[19]P. Q. Liu, I. J. Luxmoore, S. A. Mikhailov, N. A. Savostianova, F. Valmorra, J. Faist, and G. R. Nash, "Highly tunable hybrid metamaterials employing split-ring resonators strongly coupled to graphene surface plasmons," Nat Commun. **6**, 8969 (2015).

[20]S. J. Kindness, N. W. Almond, B. Wei, R. Wallis, V. Kamboj, P. Braeuninger-Weimer, S. Hofmann, H. E. Beere, D. A. Ritchie, and R. Degl'Innocenti, "Active control of electromagnetically induced transparency in a coupled plasmonic resonator array with graphene for continuous frequency control of terahertz radiation," Adv. Opt. Mater. **6**, 1800570 (2018).

[21]S. J. Kindness, N. W. Almond, W. Michailow, B. Wei, L. A. Jakob, K. Delfanazari, P. Braeuninger-Weimer, S. Hofmann, H. E. Beere, D. A. Ritchie, and R. Degl'Innocenti, "Graphene-integrated metamaterial device for all-electrical polarization control of terahertz quantum Cascade lasers," ACS Photonics **6**, 1547–1555 (2019).

[22]T. T. Kim, S. S. Oh, H. D. Kim, H. S. Park, O. Hess, B. Min, and S. Zhang, "Electrical access to critical coupling of circularly polarized waves in graphene chiral metamaterials," Sci. Adv. **3**, e1701377 (2017).

[23]S. J. Kindness, N. W. Almond, W. Michailow, B. Wei, K. Delfanazari, P. Braeuninger-Weimer, S. Hofmann, H. E. Beere, D. A. Ritchie, and R. Degl'Innocenti, "A terahertz chiral metamaterial modulator," Adv. Opt Mater. **8**, 2000581 (2020).

[24]A. J. Sabbah and D. M. Riffe, "Femtosecond pump-probe reflectivity study of silicon carrier dynamics," Phys. Rev. B **66**, 165217 (2002).

[25]T. Terashige, H. Yada, Y. Matsui, T. Miyamoto, N. Kida, and H. Okamoto, "Temperature and carrier-density dependence of electron-hole scattering in silicon investigated by optical-pump terahertz-probe spectroscopy," Phys. Rev. B **91**, 241201(R (2015).

[26]E. Hendry, M. Koeberg, J. Pijpers, and M. Bonn, "Reduction of carrier mobility in semiconductors caused by charge-charge interactions," Phys. Rev. B **75**, 233202 (2007).

[27]G. Li, D. Li, Z. Jin, and G. Ma, "Photocarriers dynamics in silicon wafer studied with optical-pump terahertz-probe spectroscopy," Opt. Commun. **285**, 4102–4106 (2012).

[28]S.-F. Shi, T.-T. Tang, B. Zeng, L. Ju, Q. Zhou, A. Zettl, and F. Wang, "Controlling graphene ultrafast hot carrier response from metal-like to semiconductor-like by electrostatic gating," Nano Lett. **14**, 1578–1582 (2014).

[29]G. Jnawali, Y. Rao, H. Yan, and T. F. Heinz, "Observation of a transient decrease in terahertz conductivity of single-layer graphene induced by ultrafast optical excitation," Nano Lett. **13**, 524–530 (2013).

[30]S. Winnerl, F. Gottfert, M. Mittendorff, H. Schneider, M. Helm, T. Winzer, E. Malic, A. Knorr, M. Orlita, M. Potemski, M. Sprinkle, C. Berger, and W. A. de Heer, "Time-resolved spectroscopy on epitaxial graphene in the infrared spectral range: Elaxation dynamics and saturation behaviour," J. Phys.: Condens. Matter **25**, 054202 (2013).

[31]A. C. Tasolamprou, A. D. Koulouklidis, C. Daskalaki, C. P. Mavidis, G. Kenanakis, G. Deligeorgis, Z. Viskadourakis, P. Kuzhir, S. Tzortzakis, M. Kafesaki, E. N. Economou, and C. M. Soukoulis, "Experimental demonstration of ultrafast THz modulation in a graphene-based thin film absorber through negative photoinduced conductivity," ACS Photonics **6**(3), 720–727 (2019).

[32]H. Sun, Y. Hu, Y. Tang, J. You, J. Zhou, H. Liu, and X. Zheng, "Ultrafast polarization-dependent all-optical switching of germanium-based metaphotonic devices," Photonics Res. **8**, 263–270 (2020).

[33]W. X. Lim, M. Manjappa, Y. K. Srivastava, L. Cong, A. Kumar, K. F. MacDonald, and R. Singh, "Ultrafast all-optical switching of germanium-based flexible metaphotonic devices," Adv. Mater. **30**, 1705331 (2018).

[34]L. Cong, Y. K. Srivastava, H. Zhang, X. Zhang, J. Han, and R. Singh, "All-optical active THz metasurfaces for ultrafast polarization switching and dynamic beam splitting," Light **7**, 28 (2018).

[35]H. T. Chen, J. F. O'Hara, A. K. Azad, A. J. Taylor, R. D. Averitt, D. B. Shrekenhamer, and W. J. Padilla, "Experimental demonstration of frequency-agile terahertz metamaterials," Nat. Photonics **2**, 295–298 (2008).

[36]P. Goulain, A. D. Koulouklidis, J. M. Manceau, C. Daskalaki, B. Paulillo, K. Maussang, S. Dhillon, J. R. Freeman, L. Li, E. H. Linfield, S. Tzortzakis, and R. Colombelli, "Femtosecond broadband frequency switch of terahertz three-dimensional meta-atoms," ACS Photonics **8**, 1097–1102 (2021).

[37]A. Kumar, A. Solanki, M. Manjappa, S. Ramesh, Y. K. Srivastava, P. Agarwal, T. C. Sum, and R. Singh, "Excitons in 2D perovskites for ultrafast terahertz photonic devices," Sci. Adv. **6**, eaax8821 (2020).

[38]O. J. Burton, V. Babenko, V.-P. Veigang-Radulescu, B. Brennan, A. J. Pollard, and S. Hofmann, "The role and control of residual bulk oxygen in the catalytic growth of 2D materials," J. Phys. Chem. C **123**, 16257–16267 (2019).

[39]J. A. Alexander-Webber, A. A. Sagade, A. I. Aria, Z. A. V. Veldhoven, P. Braeuninger-Weimer, R. Wang, A. Cabrero-Vilatela, M.-B. Martin, J. Sui, M. R. Connolly, and S. Hofmann, "Encapsulation of graphene transistors and vertical device integration by interface engineering with atomic layer deposited oxide," 2D Mater. **4**, 011008 (2016).

[40]R. Degl'Innocenti, L. Xiao, S. J. Kindness, V. S. Kamboj, B. Wei, P. Braeuninger-Weimer, K. Nakanishi, A. I. Aria, S. Hofmann, H. E. Beere, and D. A. Ritchie, "Bolometric detection of terahertz quantum cascade laser radiation with graphene-plasmonic antenna," J. Phys. D **50**, 174001 (2017).

[41]P. A. George, J. Strait, J. Dawlaty, S. Shivaraman, M. V. Chandrashekhar, F. Rana, and M. G. Spencer, "Ultrafast optical-pump terahertz-probe spectroscopy of the carrier relaxation and recombination dynamics in epitaxial graphene," Nano Lett. **8**, 4248–4251 (2008).

[42]M. Halbhuber, J. Mornhinweg, V. Zeller, C. Ciuti, D. Bougeard, R. Huber, and C. Lange, "Non-adiabatic stripping of a cavity field from electrons in the deep-strong coupling regime," Nat. Photonics **14**, 675–679 (2020).

[43]Lancaster University's PURE, https://doi.org/10.17635/lancaster/researchdata/544.